



# Investigate the Impact of the Pumping Station's Operation on the Hydrodynamic Changes of Sanhe Branch

Shaobo Wang<sup>1</sup>, Mingming Gao<sup>1</sup>, Chu Chen<sup>1</sup>, Zhiwei Wang<sup>1</sup>, Min Yu<sup>2</sup>

<sup>1</sup>Jiangsu Water Surveying and Design Institute of Water Resource Co., LTD,  
Yangzhou, 225127 China

<sup>2</sup>Yangzhou Urban River Management Office, Yangzhou, 225000 China

\*Corresponding: Shaobo Wang, e-mail: 350846165@qq.com

**Abstract.** A two-dimensional hydrodynamic model of Sanhe branch has been developed using MIKE21 software to investigate the impact of the South to North Water Diversion Project on its hydrodynamics. Design and comparative conditions have been established to analyze the hydrodynamic changes under different pumping specifications. The results indicate stable flow adjacent to the Jiangba ship lock and Jinhu pumping station, with no local blockage phenomenon. Water level changes are primarily influenced by the volume of Sanhe branch rather than pumping operations. In the critical scenario, the water level of the overflowed highway reaches 8.11m at the highest, and the water level of the lock reaches 7.55m at the lowest. The water level channel volume relationship curve obtained from model simulation can be utilized to formulate control schedules for Baoying, Jinhu, and Hongze pumping stations, providing a scientific basis for operation of the east route of South-to-North Water Diversion Project.

**Keywords:** South-to-North Water Diversion Project; watercourse of Huaihe River to Yangtze River; hydrodynamic; numerical simulation

## Introduction

### 1

With the advancement of water conservancy construction in China, an increasing number of pumping stations are being utilized. Researching the impact of pumping station operation on regional hydrodynamics has become a prominent direction. BIAN Xinsheng, et al., investigated the effects of water pumping from Jinhu Station on the hydrodynamics of the purse seine aquaculture area in Baoying Lake. They discovered that pumping led to instantaneous flow velocity peaks and suggested that staggering the activation of pumping machines at regular intervals can effectively mitigate the rapid increase in flow velocity within the study area<sup>[1]</sup>. LIN Jing-jing, et al., used Jiangnan pumping station in the Great Tangxun Lake basin in Wuhan as a case study and concluded that compared with ND, WD had a significantly increased influence range and

© The Author(s) 2025

Y. Qiu et al. (eds.), *Proceedings of the 2024 7th International Conference on Civil Architecture, Hydropower and Engineering Management (CAHEM 2024)*, Advances in Engineering Research 256, [https://doi.org/10.2991/978-94-6463-650-5\\_35](https://doi.org/10.2991/978-94-6463-650-5_35)

degree on water quality index concentration in river reach. The length and width of  $TP$  pollution zone exceeding Class II water quality standard increased by 2.66 times and 0.64 times, respectively. Additionally,  $TP$  concentration downstream Yangsigang national control section exceeded standards by 0.16 times, equivalent to AD's impact. Pumping station drainage was identified as a potential risk source for water quality exceeding standards during flood seasons<sup>[2]</sup>.

The watercourse of Huaihe River to Yangtze River serves as the primary outlet for flood control, with functions including drainage, irrigation, and shipping. This water conservancy facility plays a crucial role in safeguarding the safety of people's lives and property, as well as promoting economic development in the lower reaches of the Huaihe River. The Hongze pumping station and Jinhu pumping station are strategically located at the beginning and end of the Sanhe branch of the watercourse of Huaihe River to Yangtze River respectively, serving essential roles in water transportation for the east route of the South-to-North Water Diversion Project.

Since the implementation of the South-to-North Water Diversion Project, according to the local management department, when Jinhu pumping station operates, the nearby road has the risk of flooding. When Hongze pumping station operates, the local shipping department reflected that the pumping of large flow would cause low water level of the approach channel of Jiangba ship lock and adversely affect navigation. In order to balance the different water level requirements of the flood road and the lock approach channel, a two-dimensional hydrodynamic numerical model of Sanhe branch of the watercourse of Huaihe River to Yangtze River has been constructed using MIKE21. The hydrodynamic variation of Sanhe branch during pumping station operation has been studied.

## 2 Materials and Methods

### 2.1 Study Area

The designed flood discharge of the watercourse of Huaihe River to Yangtze River is  $12000\text{m}^3/\text{s}$ , with corresponding designed water levels of 13.95m in Zhongdu, 11.97m in Jinhu, 9.53m in Shijian, 9.33m in Gaoyou, 8.96m in Xilipu and 8.33m in Liuzha. The inflow channel consists of a series of rivers, lakes and beaches, including the new Sanhe and Jingou diversion section in the upper section, Gaoyou Lake, Xinmin Beach and Shaobo Lake in the middle section, and six rivers dividing the lower section before merging into Jiajiang River and connecting with the Yangtze River.

The total length of the watercourse of Huaihe River to Yangtze River is 157.2km, with the river beach accounting for approximately half of this distance. There are four control points along the entire route: Sanhe sluice, Jinhu, Gaoyou, and Guijiang control lines<sup>[3]</sup>. The research area is primarily focused on the section from Sanhe sluice to Jinhu pumping station in the river inlet as shown in Fig. 1.

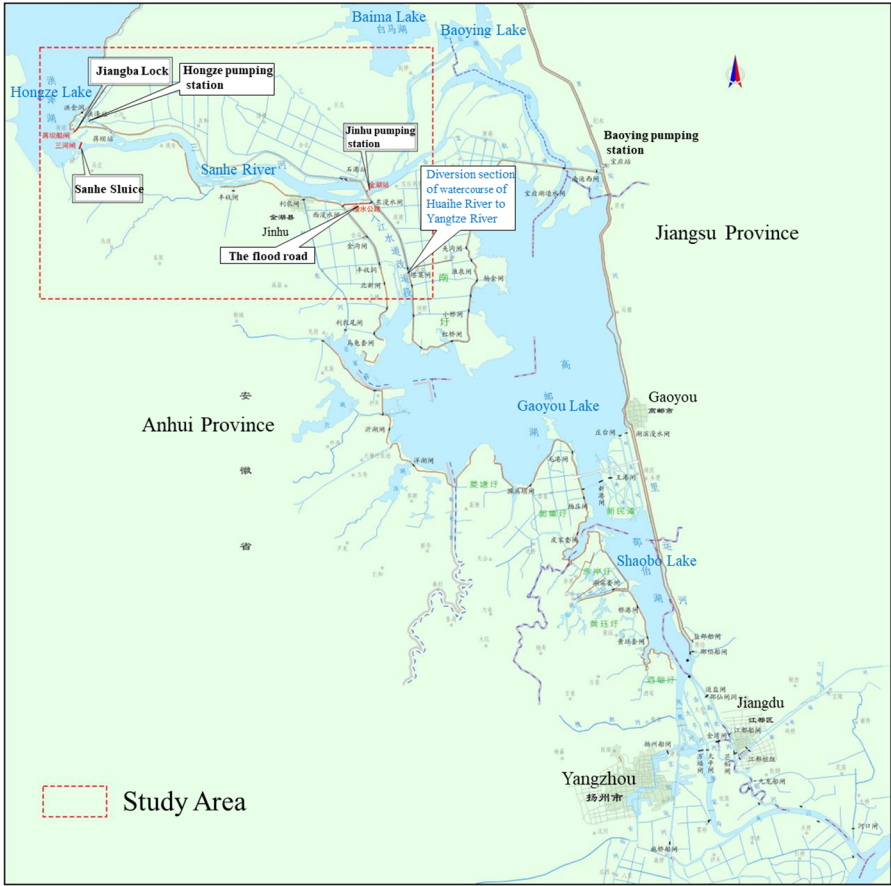


Fig. 1. Position illustration of the study area

## 2.2 MIKE21 Model

The MIKE21 model, developed by the Danish Hydraulics Institute (DHI), is the fundamental module of the MIKE software series. It utilizes the finite volume calculation method and has been widely utilized in hydrodynamic research globally<sup>[4-6]</sup>, with its numerical simulation capabilities being recognized internationally. Its primary applications include simulating lakes, rivers, reservoirs, oceans, waves, and sediment. The governing equations of the MIKE21 model are as follows:

Continuum equation:

$$\frac{\partial \varepsilon}{\partial t} + \frac{\partial p}{\partial x} + \frac{\partial q}{\partial y} = \frac{\partial h}{\partial t} \tag{1}$$

Momentum equation:

$$\frac{\partial p}{\partial t} + \frac{\partial}{\partial x} \left( \frac{p^2}{h} \right) + \frac{\partial}{\partial y} \left( \frac{pq}{h} \right) + gh \frac{\partial \varepsilon}{\partial x} + \frac{gp}{c^2 h^2} - \Omega q - fVV_x = 0 \tag{2}$$

$$\frac{\partial q}{\partial t} + \frac{\partial}{\partial x} \left( \frac{q^2}{h} \right) + \frac{\partial}{\partial y} \left( \frac{pq}{h} \right) + gh \frac{\partial \varepsilon}{\partial y} + \frac{gq\sqrt{p^2+q^2}}{C^2h^2} - \Omega p - fV V_y = 0 \quad (3)$$

Where:  $\varepsilon$  represents the water level elevation;  $p$  and  $q$  represent the flow in the  $x$  and  $y$  directions respectively;  $h$  represents the water depth;  $t$  represents time;  $g$  represents gravitational acceleration;  $C$  represents Chézy coefficient;  $\Omega$  represents Coriolis coefficient;  $f$  represents wind friction;  $V$  represents wind speed;  $V_x$  and  $V_y$  represent the components of wind in the  $x$  and  $y$  directions, respectively.

### 2.3 Model Settings

The data to be input into the two-dimensional hydrodynamic model includes: water grid data of Sanhe branch (with closed water surface boundaries), water depth and elevation data for the reservoir area, open boundary flow and water level time series data, model simulation parameters, simulated initial water level and flow, as well as simulated time and time step settings. After numerous tests, a two-dimensional hydrodynamic model suitable for Sanhe branch is obtained.

In Sanhe branch, the upstream water enters from Jinhu pumping station., The effect of opening and closing of Sanhe sluice is not considered in this simulation. Therefore, Jinhu pumping station and Hongze pumping station are set as open boundaries, and the rest boundaries are closed. Both open boundary conditions are set as flow time series. The model uses unstructured triangular mesh to divide the research area. The triangular mesh can better fit the land and water boundary of the research area, and the mesh density and mesh size can be adjusted at will.

Land and Water boundary data (land.xyz) and water depth data (water.xyz) of the study area are obtained from the latest terrain survey data. Land and Water boundary data (land.xyz) is imported into the Mesh Generator to generate the grid of the study area and set the model boundary. The number of mesh in the model is 68188, and the side length of the triangular mesh is within 10m. Water depth data (water.xyz) is imported into the grid and interpolated to generate the topographic map of the study area, as shown in Fig. 2.

Observed cross sections CS1-CS9 are distributed in the diversion rivers of Hongze pumping station, Jiangba ship lock and Sanhe sluice to monitor the change in flow, as shown in Fig. 2. The observation points T1-T3 are located on the side of the approach channel of Jiangba ship lock (on the left side of the model), used to monitor change in water level of the approach channel of the lock. The observation points T4-T6 are located on the riverside side of the flood road (adjacent to the Jinhu pumping station), used to monitor change in water level adjacent to the road.

The calculation conditions to be specified for the MIKE21 hydrodynamic model include simulation time and time step, terrain data, Krone value, wet and dry boundary specifications, eddy viscosity coefficient, as well as boundary and initial conditions.

Simulation time and time step: The hydrodynamic model has a simulation time of 80 minutes, with a time step of 120 seconds and a total of 40 steps.

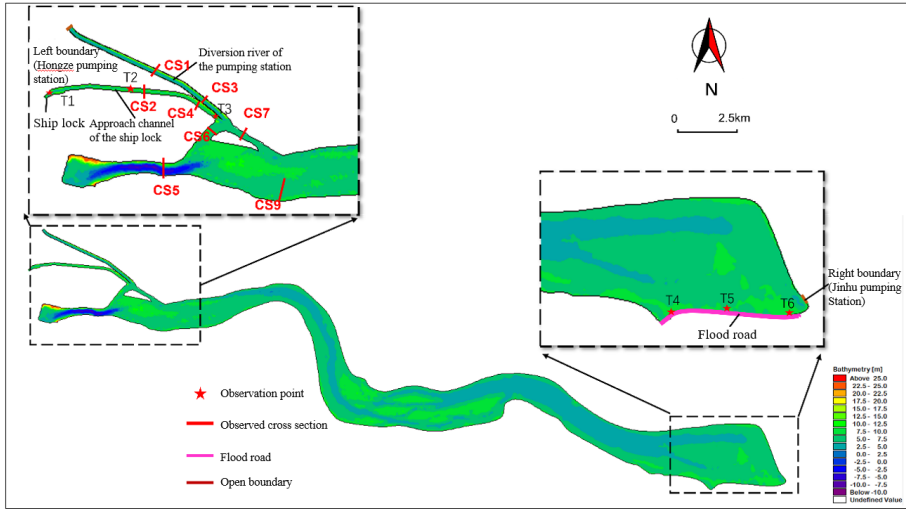


Fig. 2. Topographic map and positions of observation point

CFL number: The Krone value in the model setup is determined by grid resolution, water depth, and time step. The model can only run normally when the krone value is less than 1, so the CFL value is set to 0.8 to ensure the stability of model operation.

Flood and dry: MIKE21 has the capability to adjust calculation conditions based on the water depth of each grid and can flexibly incorporate formulas into the calculation process. The model uses dry and wet water depths to determine whether a cell grid is included in the calculation. In this model, the dry water depth is 0.001m, the submerged water depth is 0.05 m, and the wet water depth is 0.1 m.

Eddy Viscosity: Smagorinsky formula has been selected, with a value of 0.28.

Bed Resistance: The Manning coefficient Number is chosen for bed friction, considering the pertinent literature [7-8], and a numerical model roughness value of 0.026 is used in this paper. The default values are applied to other parameters.

## 2.4 Working Condition

According to the information provided by the South-to-North Water transfer management department and related literature [9]:

a. The designed pumping flow of Jinhu pumping station is  $150\text{m}^3/\text{s}$ . During the water supply period, the design station has a water level of 7.9m, with a high water level of 8.0m, a low water level of 7.5m, and an average water level of 7.65m;

b. The Hongze pumping station is designed to accommodate a pumping flow of  $150\text{m}^3/\text{s}$ . The design includes a lower water level of 7.1m, a higher water level of 7.8m, a lower water level of 7.3m, and an average water level of 7.55m;

c. The flood road has an elevation of 8m, and the storm surge is about 0.2-0.3m during the water transfer period;

d. The minimum navigable water level of the lock river is 7.15m.

**Table 1.** Boundary condition of different operation schemes

Working condition	Initial water level (m)	Left boundary flow (m <sup>3</sup> /s)	Right boundary flow (m <sup>3</sup> /s)
1	High water level during water supply period	-150	150
2		-150	0
3		0	150

Therefore, three operational conditions are established based on different operation scheduling schemes, as shown in Table 1. Working condition 1 is the design working condition, during which Jinhu and Hongze pumping stations pump at a rate of 150m<sup>3</sup>/s. Working condition 2 involves Hongze pumping station operating at 150m<sup>3</sup>/s while Jinhu pumping station does not operate. Working condition 3 entails Jinhu pumping station operating at 150m<sup>3</sup>/s while Hongze pumping station does not operate. The initial water level under the design condition can be determined by setting the left boundary as the lower water level of the design station of Hongze pumping station at 7.8m and the right boundary as the water level of the design station of Jinhu pumping station at 7.9m. After running the model until the global water surface line stabilizes, it is found that the initial water level at the entrance of the lock is approximately 7.88m, and adjacent to flood road is about 7.90m.

### 3 Results

#### 3.1 Model Verification

The hydrodynamic model of MIKE 21FM has been utilized to simulate the water area of Sanhe branch and output the flow results of the section. The measured sections, mainly located in the approach channel of the ship lock and diversion rivers of the pumping station (refer to Fig. 2 for location), are convenient for monitoring flow within the branch. The representative measured flow data can be used to validate the model.

**Table 2.** Results of model calibration

Cross section	Location	Measured discharge (m <sup>3</sup> /s)	Calculate discharge (m <sup>3</sup> /s)	MAE (m <sup>3</sup> /s)	MRE (%)
CS1	North of the diversion river of Hongze pumping station	49.83	48.812	1.018	2.04
CS2	North of the approach channel of Sanhe ship lock	0.05	0.052	0.002	4.00
CS3	South of the diversion river of Hongze pumping station	61.25	62.271	1.021	1.67
CS4	South of the approach channel	1.93	1.885	0.045	2.33

	of Sanhe ship lock				
CS5	Sanhe branch	17.27	17.545	0.275	1.59
CS6	Upper stream of Sanhe branch	44.43	45.057	0.627	1.41
CS7	North branch of watercourse of Huaihe River to Yangtze River	9.6	9.44	0.16	1.67
CS8	South branch of watercourse of Huaihe River to Yangtze River	26.54	26.829	0.289	1.09

Flow monitoring at observed cross sections took place from January 5th, 2019 to January 7th, 2019 with a maintained pumped flow of 60m<sup>3</sup>/s at Hongze pumping station and Jinhu pumping station. With error indexes of MAE (mean absolute error) and MRE (mean relative error), a comparison between simulated flows and measured flows at cross sections is presented in Table. 2.

The simulation results show a relative error of less than 2.33% and an absolute error within the range of 1.02m<sup>3</sup>/s when compared with the actual results in Table.2. Overall, the simulation demonstrates good accuracy, with errors controlled within the required range for model calculations.

### 3.2 Flow Pattern Analysis

There is a significant shoal area located between the flood road and Jinhu pumping station, which effectively impedes the inflow of water to the pumping station and serves to delay the rapid rise of water levels adjacent to the flood road. The diversion river of Hongze pumping station is connected to Sanhe branch. During operation of Hongze pumping station, there is smooth flow at the junction between its diversion river and Sanhe branch, with most pumped water coming from Sanhe branch rather than directly from the approach channel of the ship lock as shown in Fig. 3 and Fig. 4.

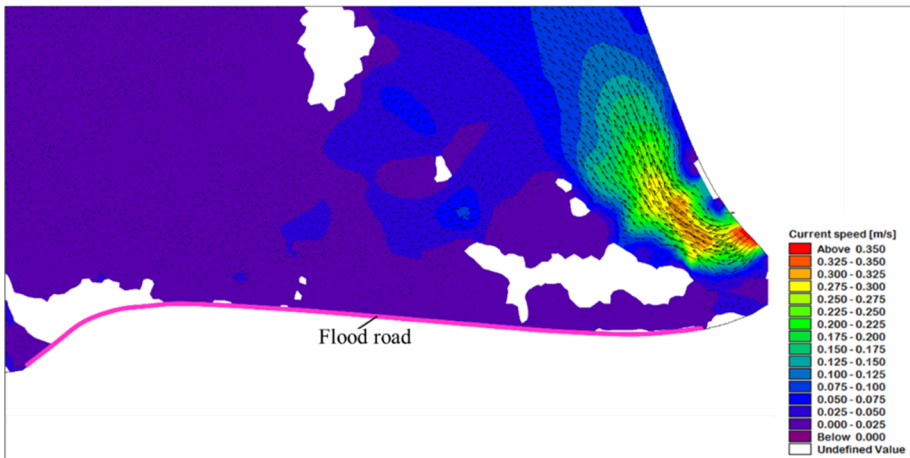
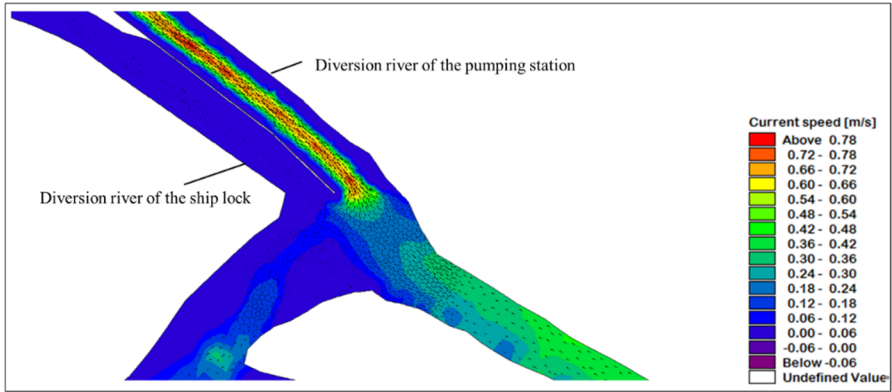
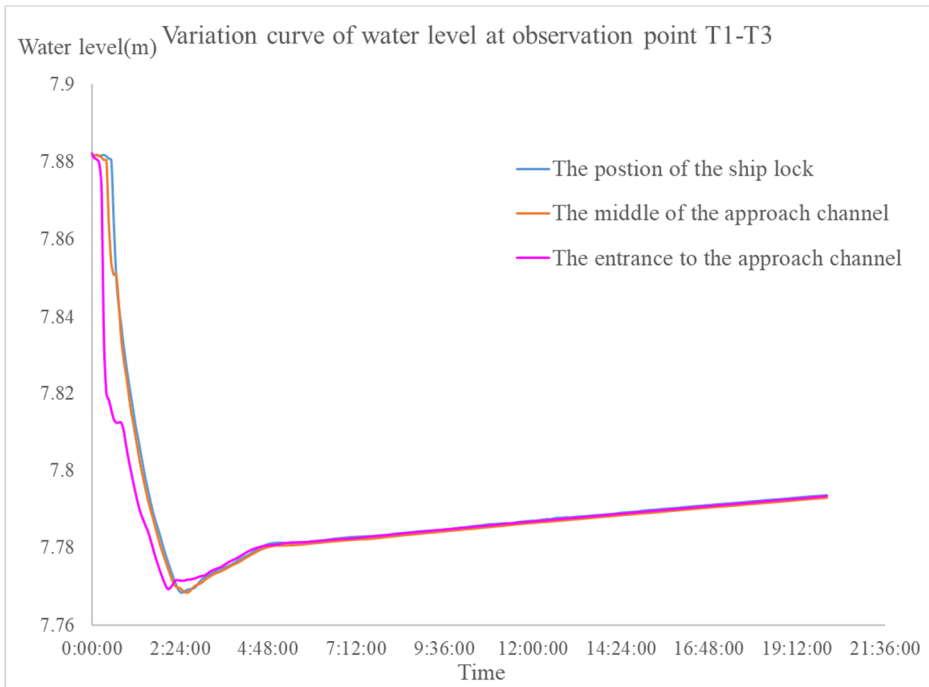


Fig. 3. Schematic diagram of flow pattern and velocity distribution adjacent to the flood road



**Fig. 4.** Distribution diagram of flow pattern and velocity of water near the approach channel of the ship lock

### 3.3 Variation Law of Water Level



**Fig. 5.** Graphic of variation curves of water level at observation point T1-T3

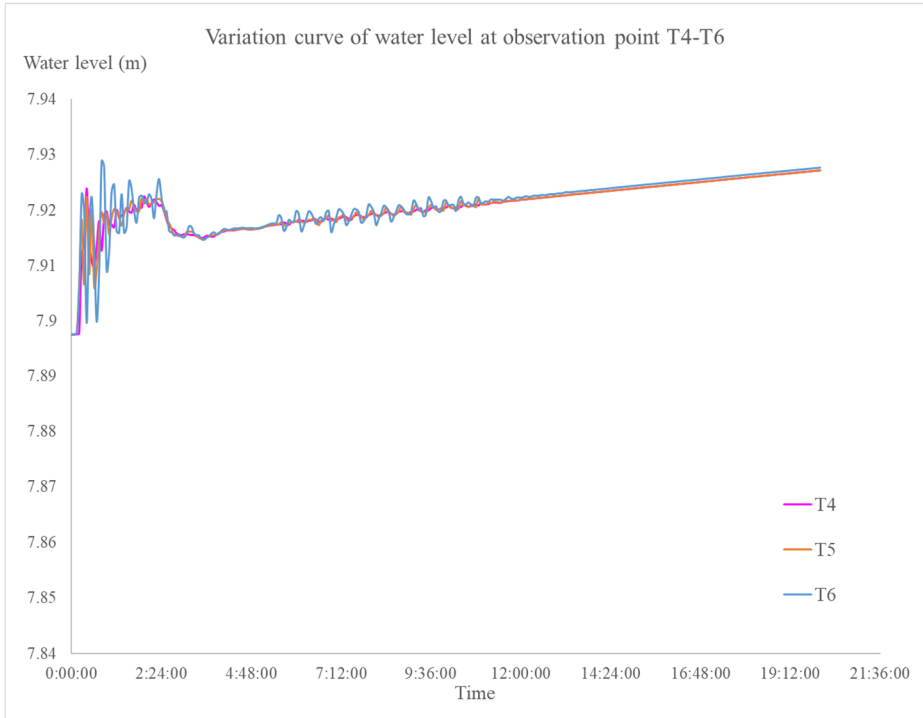


**Fig. 6.** Graphic of variation curves of water level at observation point T4-T6

Under operational conditions, Jinhu and Hongze pumping stations commence pumping operations at  $150\text{m}^3/\text{s}$  each. Based on the analysis of water levels at the observation point, as shown in Fig. 5 and Fig. 6, leakage from Hongze pumping station causes a rapid decrease in the water level of the approach channel of the ship lock 4 minutes after its operation began. Approximately 144 minutes later, with combined influence from Jinhu pumping station's diversion flow and Hongze pumping station's leakage, the water level gradually stabilizes. The difference in water levels at various points along the ship lock is minimal, resulting in smooth flow in the approach channel. After 4 minutes of operation, Jinhu pumping station led to a slight increase in water level adjacent to the flood road through diversion. About 144 minutes later, under joint influence from both Jinhu and Hongze pumping stations, the water level remains stable. The difference in water levels at each measuring point along flood road is negligible, with no local backwater present adjacent to it. Therefore, T1 and T5 accurately represent respective water levels for both approach channels of ship lock and road area.

**Water Level Adjacent to the Flood Road.** Through the analysis of three working conditions, it is evident that the water level near the flood road is primarily influenced by the net flow of the Sanhe branch section, as shown in Fig. 7.

a. Given that the Jinhu pumping station is diverting water at a designed flow of  $150\text{m}^3/\text{s}$  and the Hongze pumping station is not in operation, the net flow of the Sanhe

branch section remains at  $150\text{m}^3/\text{s}$ . After 20 hours, the channel volume of the Sanhe branch increases by  $1.08 \times 10^7 \text{ m}^3$ , resulting in a rise in water level to 8.11m at Hanoi and flood road by the lock.;

b. Given that Jinhu pumping station utilizes the designed discharge of  $150\text{m}^3/\text{s}$  for water diversion, and Hongze pumping station employs the same discharge for water pumping, the section of Sanhe branch has a discharge of 0. After 20 hours, there is a slight increase in the water level adjacent to the flood road by 0.02m.

c. Under the condition that Hongze pumping station is discharging at a designed discharge of  $150\text{m}^3/\text{s}$  and Jinhu pumping station remains inactive, the net flow in the section of Sanhe branch is  $-150\text{m}^3/\text{s}$ . After 20 hours, the channel volume in the section of Sanhe branch decreases by  $1.08 \times 10^7 \text{ m}^3$ , causing the water level adjacent to the flood road to drop to 7.71m.

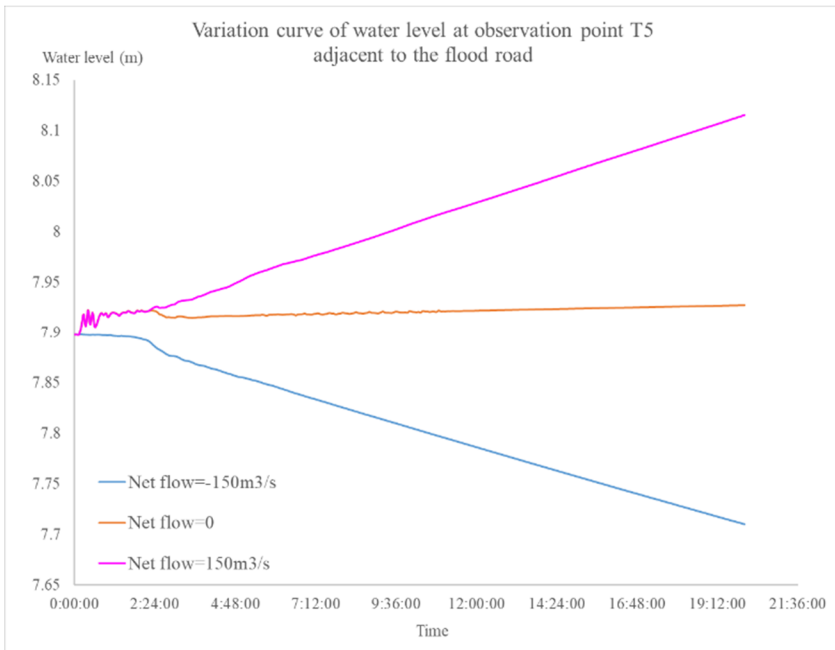


**Fig. 7.** Graphic of variation curves of water level at observation point T5 adjacent to the flood road

**Water Level of the Approach Channel of the Ship Lock.** Through the analysis of the high water level condition during the water supply period, it can be seen that the water level of the ship lock is mainly affected by the regional net flow as shown in Fig. 8.

a. The Hongze pumping station does not operate under the following conditions at the Jinhu pumping station with a design flow of  $150\text{m}^3/\text{s}$ : During the period of 0-2h24min operation, the average regional net flow is 0 and the regional channel volume remains unchanged. The slight rise in water level can be disregarded. During

2h24min-20h operation, the average regional net flow is  $0.8\text{m}^3/\text{s}$  and the regional channel volume increased by  $56,800\text{m}^3$ . The water level rise to  $8.1\text{m}$ .

b. During the 0-2h24min operation, the average regional net flow at Jinhu pumping station is  $-3.2\text{m}^3/\text{s}$ , with a designed flow of  $150\text{m}^3/\text{s}$ , and at Hongze pumping station with the same flow. The regional channel volume decreases by  $27,700\text{m}^3$ , resulting in a water level decrease to  $7.78\text{m}$ . During the period of 2h24min-20h operation, the average regional net flow is 0 at both stations, leading to minimal change in the regional channel volume and a slight increase in water level that is negligible.

c. During the initial operation period from 0-2h24min with a design discharge of  $150\text{m}^3/\text{s}$  at Hongze pumping station and consistent pumping operations, there is an average negative net flow of  $-3.2\text{m}^3/\text{s}$  within the region resulting in a depletion of  $27,700\text{m}^3$  from the regional channel volume and causing a decline in water level to  $7.78\text{m}$ ; Subsequently during the period from 2h24min-20h operation, there is an average negative net flow of  $-0.95\text{m}^3/\text{s}$  leading to a reduction of  $61,000\text{m}^3$  in regional channel volume and causing further decrease in water level to reach as low as  $7.55\text{m}$ .

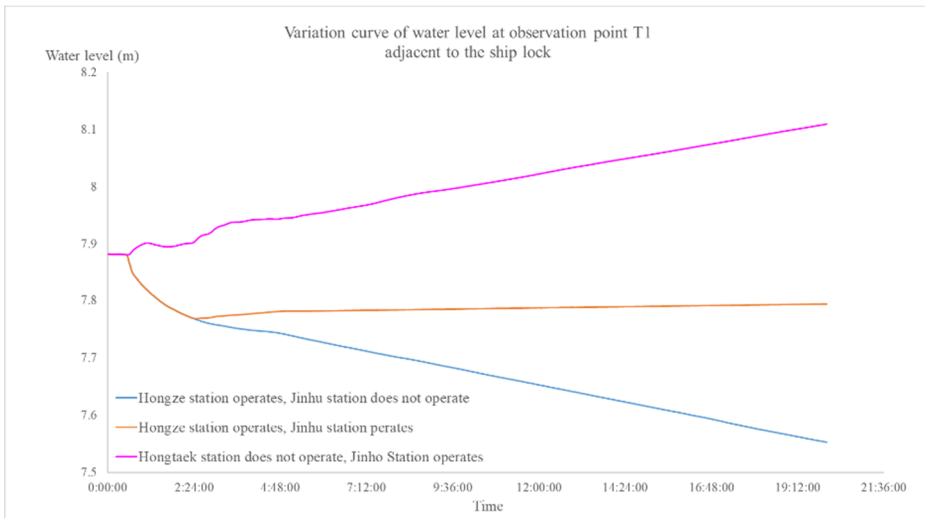


**Fig. 8.** Graphic of variation curves of water level at observation point T1 adjacent to the ship lock

### 3.4 Rate of Water Level Change

**Water Level Adjacent to the Flood Road.** The analysis above indicates that the water level of the area adjacent to the flood road is not directly influenced by the pumping station, and extracting water from the station will not directly result in a change in its water level. The water level of the flood road is primarily impacted by the overall water level of the Sanhe branch section and the volume of the Sanhe branch, therefore, studying the rate of water level change can be achieved by establishing a water-volume relationship curve for this section (refer to Fig. 9).

$$t = \frac{V_g - V_p}{Q_{\text{net}}} \quad (4)$$

$$Q_{\text{net}} = Q_{\text{in}} - Q_{\text{out}} \quad (5)$$

Where  $t$  represents the time required for the water level of the flooded road to rise or fall to the target water level;

$V_p$  and  $V_g$  denote the current channel volume and the channel volume under the target water level, respectively. The channel volume can be measured using a specific figure depicting the relation curve between water level and channel volume;

$Q_{\text{net}}$  stands for the net flow of the Sanhe branch section, while  $Q_{\text{in}}$  and  $Q_{\text{out}}$  represent the diversion flow of Jinhu pumping station and pumped flow of Hongze pumping station, respectively.

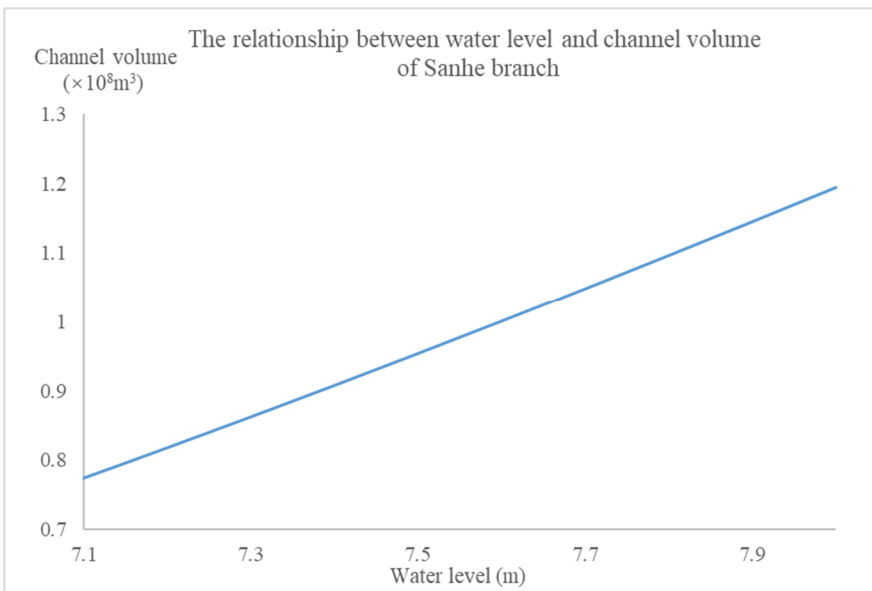


Fig. 9. Graphic of the relationship between water level and channel volume of Sanhe branch

**Water Level of the Approach Channel of the Ship Lock.** The fluctuation in water level of the approach channel to the ship lock is primarily influenced by the local water level of the Sanhe branch section and the capacity of the channel. Therefore, analyzing the correlation curve between the local water level and the channel capacity of the lock inlet river (refer to Fig. 9) can assist in determining the duration required for changes in water level.

$$t = \frac{V_g - V_p}{Q_{\text{net}}} \quad (6)$$

$$Q_{\text{net}} = Q_{\text{in}} - Q_{\text{out}} \quad (7)$$

Where  $t$  represents the time required for the water level to rise or fall to the target level;

$V_p$  and  $V_g$  denote the current volume of the diversion river channel and the volume of the diversion river below the target water level, respectively. The channel volume can be determined from the relationship curve between water level and diversion river volume in Fig. 10;

$Q_{net}$  is the net flow channeled by the lock, while  $Q_{in}$  and  $Q_{out}$  represent inflow and outflow of water into and out of the lock, respectively.

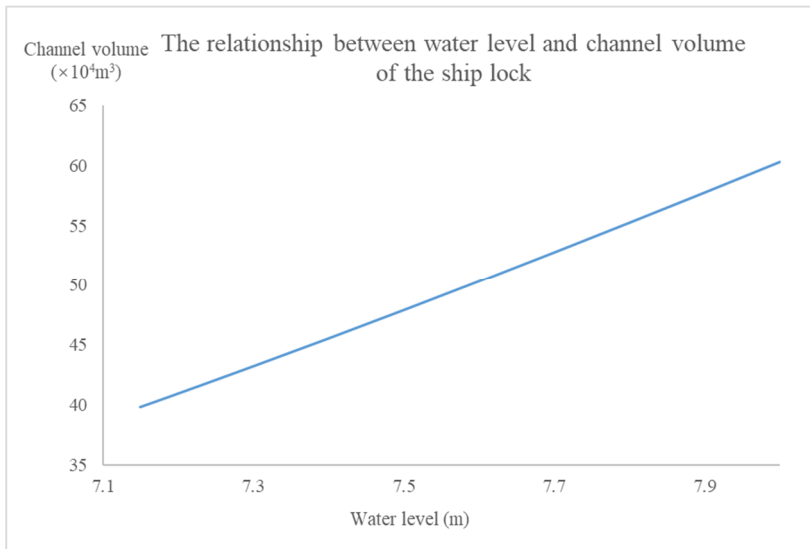


Fig. 10. Graphic of the relationship between water level and channel volume of the ship lock

## 4 Discussion

### 4.1 Model Performance

In the model setting, due to the uniform values assigned to all relevant parameters such as bed resistance and eddy viscosity across the entire study area, there was a certain level of error in the model's accuracy. Upon comparison analysis between the simulation results and measured data, it was found that the relative error of the model fell within 2.33%, with an absolute error within 1.02  $\text{m}^3/\text{s}$ . Overall, the simulation error remained within acceptable limits for model calculations, indicating that the model setting was reliable and capable of simulating real-world scenarios to a satisfactory degree.

### 4.2 Countermeasure

By simulating the pumping and diversion conditions of pumping stations under various initial water level scenarios, in conjunction with studying and calculating the

channel volume and net flow of the river under different pumping station operation schemes. It is possible to determine the time required for different initial water levels to reach or fall below the critical warning level (7.8m) of the flood road (refer to Table 3). This table can serve as a guide for local pumping station management departments in proactively scheduling pumping station operations to ensure the safety of the flood road.

**Table 3.** Time required for the current water level to rise/fall to the critical water level of the flood road dike (h)

Water level(m) \ Flow (m <sup>3</sup> /s)	-37.5	-75	-112.5	-150	37.5	75	112.5	150
8.0	72.5	36.3	24.2	18.1				
7.9	36.1	18.0	12.0	9.0				
7.85	18.0	9.0	6.0	4.5				
7.75					18.2	9.1	6.1	4.6
7.7					35.7	17.8	11.9	8.9
7.6					70.9	35.4	23.6	17.7
7.5					105.6	52.8	35.2	26.4
7.4					139.8	69.9	46.6	34.9
7.3					173.4	86.7	57.8	43.4
7.2					206.5	103.2	68.8	51.6
7.1					238.9	119.5	79.6	59.7

**Table 4.** Time required for the current water level to rise/fall to the lowest navigable water level of the ship lock (h)

Water level(m) \ Flow (m <sup>3</sup> /s)	-37.5	-75	-112.5	-150	37.5	75	112.5	150
7.5	75.50	24.3	14.0	10.33				
7.4	46.27	10.66	5.36	3.00				
7.3	22.27	8.60	4.00	1.75				
7.2	1.50	1.38	1.15	1.00				
7.1					16.70	9.23	6.33	5.50
7.0					48.34	24.66	16.77	12.83

Similarly, the time required for different initial water levels to rise or fall to the lowest navigable water level of the ship lock (7.15m) can be determined by simulating pumping conditions at pumping stations under varying initial water levels. This involves studying and calculating the volume of the approach channel of the ship lock and analyzing the net flow of the approach channel under different pumping station operation schemes (refer to Table 4). The information from this analysis can be utilized to assist the local pumping station management department in scheduling pumping stations in advance, ensuring that low water levels do not hinder navigation of the ship lock.

## 5 Conclusion

This paper utilizes the MIKE21FM model to establish a two-dimensional hydrodynamic numerical model of the Sanhe branch and conducts verification and analysis of specific cross sections. The simulation results demonstrate good agreement with required calculations, indicating accurate hydrodynamic simulation. Based on these verification results, simulation analysis is conducted under three working conditions to draw conclusions about the impact of pumping station operations on the hydraulic power of Sanhe branch under different operation scheduling schemes.

(1) There is no local backwater phenomenon observed in the water area adjacent to Jiangba ship lock and Jinhu pumping station.

(2) The change of water level is minimally impacted by the operation of pumping stations, and is primarily influenced by the channel volume of Sanhe branch.

(3) The regional hydrodynamic law derived from the analysis can be utilized to optimize operational decisions for the step-pumping stations.

## Acknowledgments

This research is supported by Research project on operational capacity analysis and control operation mode of Jiangsu Section of the first phase of the East Route of South-to-North Water Diversion Project.

## References

1. Bian, X.S., Wu, M.T., Wang, X.S., et al. (2022) Analysis of the impact of water pumping from Jinhu Pumping Station of South-to-North Water Diversion on the hydrodynamics of the purse seine aquaculture area in Baoying Lake. *Jiangsu Water Resources*, 2022,(10):18-22.DOI:10.16310/j.cnki.jssl.2022.10.015.
2. Lin, J.J., Zhang, M., Huang, X.L., et al. (2024) Influence of Dainage Pumping Station on Water Quality of the Yangtze River Main Stream: Take Jiangnan Pumping Station in Wuhan as An Example. *Resources and Environment in the Yangtze Basin*, 2024,33(07):1550-1562.

3. Huo, Z.Y., Chu, E.G., Wang, B. (2021) Analysis of flood discharge capacity of control section of SanheSluice of Huaihe River watercourse entering the Yangtze River. *Jiangsu Water Resources* 08 (2021): 60-62+66. doi:10.16310/j.cnki.jssl.2021.08.016.
4. Hoque, M.A., Perrie, W., Solomon., S.M. (2017) Evaluation of two spectral wave models for wave hindcasting in the Mackenzie Delta. *Applied Ocean Research*, 62: 169-180. <https://doi.org/10.1016/j.apor.2016.11.009>.
5. Papadimitriou, A., Tsoukala, V. (2024) Evaluating and enhancing the performance of the K-Means clustering algorithm for annual coastal bed evolution applications. *Oceanologia*, 66(2): 267-285. <https://doi.org/10.1016/j.oceano.2023.12.005>.
6. Mitra, A., Kumar, V.S., Jena, B.K. (2020) Tidal characteristics in the Gulf of Khambhat, northern Arabian Sea – based on observation and global tidal model data. *Oceanologia*, 62(4): 443-459, <https://doi.org/10.1016/j.oceano.2020.05.002>.
7. Rao, G.K., Wang, L.L., Xu, J., et al. (2023) Study on the effect of wind field on hydrodynamic water quality of shallow lakes inHuaihe River watercourse entering Yangtze River during the water diversion period. *Journal of Hohai University (Natural Sciences)*, 2023, 51 (03): 31-37. <https://link.cnki.net/urlid/32.1117.TV.20220628.1715.006>.
8. Dong, X.Y., Wang L.L., Tang, H.W, Hu, Z.J., Zeng, C. (2015) Study of hydrodynamic numerical simulation of watercourse of Huaihe River to Yangtze River. *Yangtze River*, 2015,46(03):14-17. DOI:10.16232/j.cnki.1001-4179.2015.03.004.
9. Shen, M.X. (2017) Study on the influence of power generation operation at Hongze pumping station on the East line of South-to-North Water Transfer. *Resources Economiza-tion & Environmental Protection*, 2017(10): 63+65. DOI: 10.16317/j.cnki.12-1377/x.2017.10.033.

**Open Access** This chapter is licensed under the terms of the Creative Commons Attribution-NonCommercial 4.0 International License (<http://creativecommons.org/licenses/by-nc/4.0/>), which permits any noncommercial use, sharing, adaptation, distribution and reproduction in any medium or format, as long as you give appropriate credit to the original author(s) and the source, provide a link to the Creative Commons license and indicate if changes were made.

The images or other third party material in this chapter are included in the chapter's Creative Commons license, unless indicated otherwise in a credit line to the material. If material is not included in the chapter's Creative Commons license and your intended use is not permitted by statutory regulation or exceeds the permitted use, you will need to obtain permission directly from the copyright holder.

